



Evaluation of High Capacity Helical Piles in Silty-Clay Soil

Farhad Nabizadeh ^{a,*}

^aDepartment of Civil Engineering, Islamic Azad University of Chalous, Iran

Article History: Received date: 28 December 2021; revised date: 30 January 2022; accepted date: 26 February 2022

Abstract

Helical piles have been extensively used as a deep foundation system for small to large load ranges and are thus suitable for various applications. Therefore, a concern over qualifying and quantifying their axial bearing capacities and performance characteristics seems to be warranted. This paper discusses design considerations, installation procedures, and results of full-scale field load tests. In this study, axial static loading tests on single, double, and triple helix helical piles under grouted and un-grouted conditions have been conducted. The field study has been performed on silty-clay soil, to investigate the behavior of helical piles. Also, the results of the piles load tests were interpreted using six methods presented in literature to predict the ultimate load capacity (Q_u) for each pile. Results showed that in the silty-clay soil, grouted and un-grouted helical piles had a similar performance while grouted piles showed greater axial compressive strength. According to various limit load methods evaluation, it was concluded that the values for two methods of Chin, Decourt were close to the site values. © 2017 Journals-Researchers. All rights reserved

Keyword: Capacity, Helical piles, Field Study, Post Grouting

1. Introduction

Helical piles are used in the construction of structures such as buried pipelines, telecommunication and transmission towers, machine foundations, as well as commercial and residential buildings which might be exposed to uplift forces [1,2]. Among their construction and performance advantages over the conventional concrete and steel piles, one can mention their light weight, high compressive and uplift capacities, short installation time with minimal noise and vibration levels, suitability for construction

in limited access conditions, installation in frozen or swampy soil conditions, cost-effectiveness, and provision of overturning and uplift stability immediately after installation due to the elimination of the curing that is encountered in concrete anchors [3].

Another advantage of helical piles, which makes them ideal for urban areas, is that they do not cause loud noises during installation process.

The helical piles' axial capacities can be assessed analytically via either the individual bearing or cylindrical shear methods. The assumption of the individual bearing method is that bearing failure happens at each individual helix. The assumption of

* Corresponding author. Tel.: +989113914437; e-mail: f_nabizadeh2002@yahoo.com.

the cylindrical shear method is the formation of a cylindrical shear failure surface which connects the uppermost and lowermost helixes. The axial capacity of this cylindrical shear failure surface is the sum of shear resistance along the cylindrical surface, bearing resistance above the top helix (for uplift loading) and bearing resistance below the bottom helix (for compression loading), as well as adhesion along the top portion of the steel shaft above the helix level.

Byrne et al. indicated the possibility of using large diameter helical piles for offshore wind turbines, for which there are many advantages [4]. Abdelghany et al. reported a significant increase in anchor shaft's resistance to buckling and additional corrosion protection for the grouted column [5].

In this study, the behavior of helical piles in silty clay was investigated through a field study on the piles with different numbers of helixes. Also, the effect of post-grouting on the strength of these piles was assessed. The specific objectives of this study were: (1) to estimate axial compressive and tensile capacities, (2) to assess grouting effect on helical piles, (3) to compare axial compressive capacities of the helical piles. In order to achieve these objectives, six full-scale load tests were conducted including axial compressive tests. A report of the testing program is presented in the next sections.

2. Testing Procedure

2.1. Geotechnical Condition

The pile test was performed in a site in the city of Sari located in the north of Iran. The geotechnical study was conducted in the site and standard penetration (SPT) and cone penetration (CPT) tests were carried out. Soil stratigraphy in the test site consisted of silty-clay layers with middle layers of sand extended to the depth of 30 m, underlain by stiff layers of silt and clay extended to the depth of 40 m. A rock layer ranging from sandstone to soft siltstone was encountered at the depths of greater than 40 m. Ground water level was 0.5 m below the existing ground surface. The soil properties are summarized in Table 1.

Based on the test results, which were for the piles up to 28 m deep, the N-value derived from SPT was 20 and it reached 30 at deeper parts. Also, CPT results showed that at the depth of greater than 20 m, cone penetration resistance was about 5884 kPa and cone friction resistance ranged from 196 to 392 kPa.

2.2. Pile Installation and Test Set-up

Field behavior of the helical piles was studied by assessing the piles with one, two, and three helixes and the length of 6m. Also, the effect of post-grouting on the behavior of the piles was evaluated using the piles with the shaft diameter of 117 mm and helix diameter of 250 mm. The configurations for different piles considered for the helical pile load test program are summarized in Table 2. The configurations of typical test helical piles and double helix pile used in this study are shown in Figures 1&2.

The helical pile shaft was turned into the ground by torsion using a truck mounted auger or hydraulic torque motor attached to a hydraulic machine. A photograph showing installation equipment is shown in Figure 3.

Installation begins by attaching the helical pile lead section to the torque motor using a drive tool and drive pin. The lead section should be positioned and aligned at the desired location and inclination. Next, axial force should be applied to push the pilot point into the ground and the plumpness and alignment of the torque motor should be checked before rotation begins. Then, the pile should be advanced to the soil in a smooth and continuous manner at a rate of rotation typically less than 30 rpm. Installation torque and depth should be recorded at the selected intervals. Constant axial force should be applied while rotating helical piles to the ground. Helical piles are generally advanced until the termination criteria are satisfied. Termination criteria for helical piles involve achieving the required final installation torque and obtaining the minimum depth [6].

Table 1: Summary of soil properties

Depth(m)	Soil description	SPT N-value	Total unit weight (kN/m ³)	Undrained shear strength (kPa)	Frictional resistance angle (°)
0-10	Silty clay layers with middle layers of sand	22	14.2-15.2	12-20	18~20
10-20	Silty clay layers with middle layers of sand	24	14.7-15.7	15-20	18~20
20-30	Silty clay	17	15.7-16.7	20-30	15~17
30-40	Silty clay	30	16.2-17.2	25-35	15~17
> 40	Silty clay	> 50	16.7-17.7	40-60	16~20

Table 2: Summary of pile configurations

	No. of helices	Shaft diameter, (mm)	Helix diameter(mm)	Helix thickness(mm)	Prototype anchor depth (m)
Pile	1	117	250	6	6
Pile	2	117	250	6	6
Pile	3	117	250	6	6

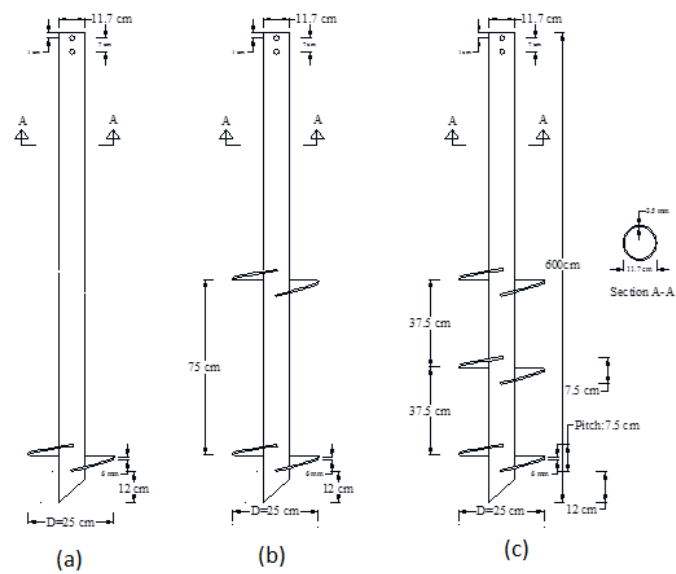


Figure1: Typical test helical piles configurations, a) single helix pile; b) double helix pile; c) triple helix pile



Figure 2: The piles used in this study



Figure 3: Helical pile installation equipment

The axial compression load tests were carried out in accordance with ASTM standards D 1143-07. Since the main objective of the load tests was to determine the ultimate bearing capacity of the pile, Procedure A (Quick Test) was adopted for all the tests wherein numerous small load increments were applied and maintained constant over short time intervals [7].

The following specific test procedures using Procedure A for Quick Tests for the piles under axial compressive or uplift loads were applied:

1. Apply test loads in the increments equal to 5% of the anticipated failure loads and maintain load constant for 5 min. Monitor movements using LDTs at the intervals of 30 sec.
2. Add load increments until reaching a failure load, but do not exceed the safe structural capacity of the pile or reaction apparatus.
3. Unload the test pile in five increments and hold for 5 min with the same monitoring intervals as for loading. A photograph showing axial compression load test is shown in Figure 4(a,b&c).



(a)



(b)



(c)

Figure 4: Test Set-up(a,b,c)

2.3. Post-grouting Operation

The primary purpose of grouting is to compact the soil under and around the pile point. In the grouting procedure, cement grout is placed around the shaft to fill the annulus created by the anchor connection couplings while being screwed into the soil to make the shaft connecting the anchors stiffer [8]. Grout is the most important component in grouted helical piles.



Figure5: a) Helical piles grouting operation b) Grouting pump

The ideal grout has a fine aggregate, such as silica fume (5-20% by weight), to increase the density and

flow ability of the grout, is liquid enough to flow down around the pile shaft, and should bond to the anchor shaft so that skin friction capacity can be achieved.

In order to perform grouting, holes were made on the pile body. With plugging the top of the pile using the packer and creating some holes on the pile body from top to tip, grouting was made throughout the pile body. Using several separate grout flow paths provided a system that did not stop grouting operation. Grout is usually a mixture of water and cement with the water-to-cement ratio (W/C) of 0.4 to 0.55. Portland cement type II was thoroughly mixed with water in a colloidal mixer. The grout was compressed using a simple pump. In a condition that the pile provides an adequate reaction for the frictional resistance, pressure at the top of the pile can be achieved at 311 psi. A typical view of grouting operation is shown in Figure 5.

3. Review of methods of interpretation of the load test results

The methods of interpretation of the load test results depend on the limit or ultimate load which can be predicted by mathematical or graphical techniques. So determining the limit or ultimate load as accurate as possible is very important. There are six methods that can be used to predict the pile capacity from load-movement records of static loading tests. A summary of these methods is presented in this section.

3.1. Davisson's Method

Davisson's Offset Limit Method (ultimate load) offers the benefit of allowing the engineer, when proofing a pile for a certain allowable load, to determine in advance the maximum allowable movement for this load with consideration to the length and size of the pile. The pile load settlement curve is plotted to a convenient scale, so that the line represents the relationship between the load and shortening of an elastic free axially loaded column, Δ makes an angle of about 20 degrees with the load axis. It can be calculated from following equation:

$$\Delta = Q L / A E \quad (1)$$

Where, Q is the applied load, L is the length of the pile, A is the cross section area of the pile, and E is the modulus of elasticity of pile material. The offset limit load straight line is plotted parallel to the elastic line to intersect the load movement curve. Where OC is given by:

$$OC = 3.8 + D / 120 \quad (2)$$

Where, D is the pile diameter in mm. The load movement curve intersects the line at point C, the ordinate of which is 0.9 Qu according to the ECDF. This method provides a failure load value that tends to be conservative without dividing by the factor of 0.9 according to the ECDF that reduces the conservatism of the method. A primary advantage of this method is that the actual limit line can be drawn on the load movement diagram already before starting the test. The offset limit load criterion is primarily intended for interpretation of quick testing methods, but it can also be used when interpreting results from the slow methods. It is not suitable for testing methods that involve loading and unloading cycles. The Davisson Offset Limit is very sensitive to errors in the measurements of load and movement and requires well-maintained equipment and accurate measurements. However, it is easy to apply and has gained wide acceptance. The disadvantage of the offset limit load lies in the difficulty of determining the modulus of elasticity E for concrete piles and concreted pipe piles.

3.2. Chin-Kondner and Modified

Chin Methods Chin assumes that the relationship between load and settlement is hyperbolic. In this method each settlement value is divided by its corresponding load value. These are plotted against the settlement. The plotted values lie on a straight line approximately. The inverse slope of the straight line indicates Chin–Kondner Extrapolation Limits. This method was used to determine the loadmovement curve for which the Chin-Kondner plot is a straight line throughout. The calculated curve is shown in Figure 4 and it is given by the following equation:

$$S/Q = C1 S + C2 \quad (6)$$

Where: S = settlement of pile at pile load Q; C1, and C2 = slope and Y-axis intercept of the straight line, respectively. The Chin-Kondner limit load is of interest when judging the results of static loading tests, particularly in conjunction with the values determined according to Davisson's and Hansen's methods. Chin's method is affected by the limit of loading, as the pile is loaded near failure the greater predicted value of ultimate load, if the last two readings are omitted the resulting ultimate load value will be reduce by about 4%. Note that some analysts use the Chin-Kondner Extrapolation Limit as the pile capacity, after applying a suitably large factor of safety, this approach is not advisable. One should not extrapolate the results when determining the allowable load by dividing the extrapolated capacity by a factor of safety. Therefore, the ECDF, Part 4, 1991 reduces the resulting Chin-Kondner Extrapolation ultimate load by dividing it by 1.2.

3.3. Mazurkiewicz's Method

Bengt (1980) suggested this method which is based on the assumption that the load–settlement curve is approximately parabolic. A series of equal pile head settlement lines are arbitrary chosen using equal intervals and the corresponding loads are marked on the abscissa, as shown in Figure 5. For the marked loads on the load axis, a 45-degree line is drawn to intersect with the next vertical line running through the next load point. These intersections fall approximately on a single straight line, the intersection of this line with the load axis defines the ultimate failure load. Smaller settlement interval may introduce more accurate results.

3.4. De Beer's method

In this method, the load–settlement values were plotted on a double logarithmic chart. When the values fall on two approximately straight lines, the intersection of these defines a limit load that is considered a pile yielding load. The method is illustrated in Figure 6 for pile no. 1, as an example pile. Regarding the results a new definition must be introduced for this method namely yielding limit

load. All previously mentioned methods determine a failure load except De Beer. Therefore, one should distinguish between the failure load and the limit load to adopt the proper factor of safety. The pile failure load, which predicted from load–settlement relationships of piles loaded to pre-failure are based on assuming certain shapes of these relationships independent of pile geometry, soil properties, and rate of loading. But the limit load is the load at which the curve begins to be steeper sloped and enters into the plastic behavior zone. This method needs the pile to be loaded near failure, because when the pile is not loaded near failure, the plotted values of the load settlement fall on approximately one straight line and the limit load is not defined.

3.5. Decourt's Extrapolation Method

This method is applied by dividing each load by its corresponding movement and plotting the resulting values against the applied load. Figure 7 shows the result for pile no. 26, as an example pile. The part of the curve that tends to a straight line intersects the load axis. Linear regression over the apparent straight-line determines the required slope $C1$ and y- intercept $C2$ constants. Decourt's ultimate load is the value at the intersection with the load axis, Decourt's ultimate load Q_u can be accurately calculated as the ratio between the y- intercept and the slope of the line as given in Eq. 7.

$$Q_u = C2 / C1 \quad (7)$$

4. Results and Discussion

As mentioned, 6 single-helix, double-helix and triple-helix piles have been constructed in two sites including silty-clay, among which 3 of these 6 piles were used without grouting and 3 of them were used with grouting. The helix spacing to diameter ratio (S/D) was 1.5 and 3 for triple helix and double helix piles, respectively. The load displacement curves are shown in Figures 6 to 10 in comparison with the axial compressive load capacities of the piles tested under grouted and un-grouted conditions.

The results showed that in single-helix piles in silty-clay, compressive capacity increased by approximately 8% after grouting. Similar to the single-helix piles, the pile resistance has increased by about 10% in the double-helix piles. But, in the triple-helix piles, the final load has been increased by about 28% after grouting. The reason was the vast disturbance of the soil around the triple-helix piles, which showed an increase after grouting due to the influence of slurry in the soil around resistance.

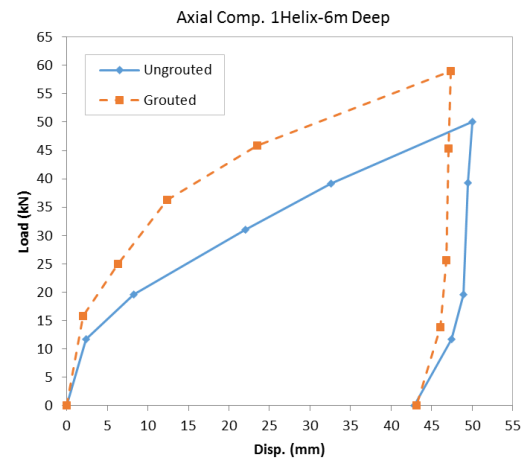


Figure 6: Axial compression load test on piles with one helix in silty-clay

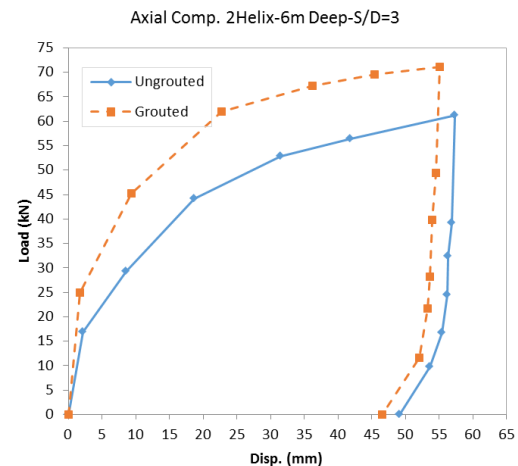


Figure 7: Axial compression load test on piles with two helixes in silty-clay

Generally, load-displacement curves can be divided into three main sections: the first part is done with displacement of about 2 mm linearly and, afterwards, a non-linear component that varied from 35 to 55 mm. It can be seen from the curves that the grouted piles in silty-clay soil have less displacement than the piles without grouting indicated that grouting operation caused an increase in pile resistance. In silty-clay soil, non-grouting triple-helix pile's bearing

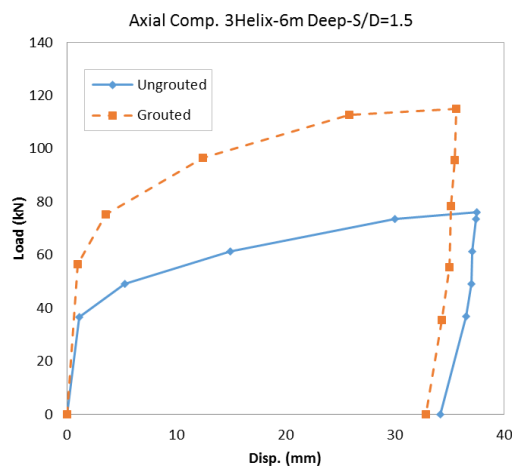


Figure 8: Axial compression load test on piles with three helices in silty-clay

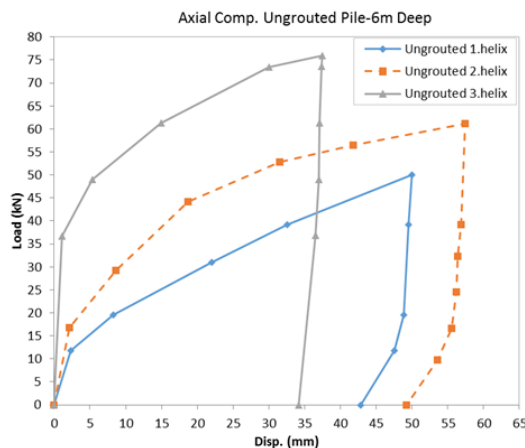


Figure 9: Axial compression load test on un-grouted piles in silty-clay

capacity was more than that of single and double-helix piles. A possible reason for this discrepancy could be that the triple-helix piles had cylindrical performance, and single and double-helix piles had individual performance; therefore, the increased number of helices resulted in the increased capacity of loading and pile stiffness. In the un-grouted piles, there was no expected pile frictional resistance due to shallow depth and low levels of tension, but when the grouting was done, the resistance increased due to adhesion. Among the grouted piles, triple-helix piles were more effective because the soil of the upper part was scrapped and grouting filled the cracks and with a further adhesion increase gives greater load capacity.

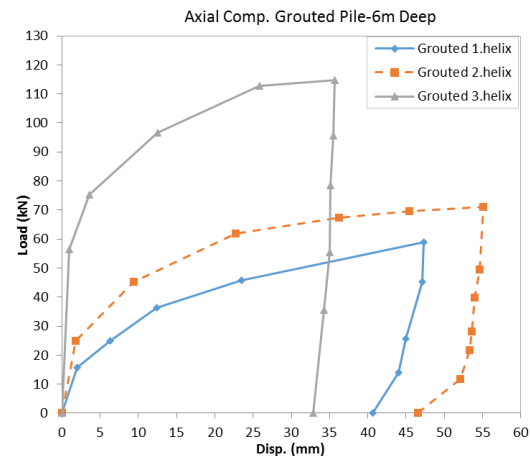


Figure 10: Axial compression load test on grouted piles in silty-clay

Generally, grouting operation in clay had compaction performance, so loading capacity increased.

Furthermore, as can be seen, when comparing load-displacement curves between the grouted and un-grouted helical piles, the data showed that both types of piles had a similar performance and the trend of both types of grouted and un-grouted axial compression load test curves are the same while grouted piles show greater axial compressive strength. The grouted helical piles deflected less at the failure load than the un-grouted ones. This stiffer

response was also very useful in structural support applications.

4.1. Estimation of Ultimate Load from Pile Load Test

A database of six axial static loading tests on single, double and triple helix helical piles under grouted and un-grouted conditions was compiled. The ultimate load capacity Q_u for each pile test was predicted using the six different interpretation methods stated in section 3 that are used in the evaluation of the pile load test. A summary of predicted ultimate failure loads is presented in Table 3.

All six tests conducted at the site were assessed to achieve the ultimate load. The ultimate load values obtained for each pile using various methods discussed earlier is presented in Table 3.

As it can be seen from Table 3, the values determined using De Beer's and Davisson's methods are the lowest ones. This is because Davisson's, and DeBeer's methods need the pile to be loaded to failure to be applicable and they were proposed to determine the limit load.

Choosing the best criteria for pile axial load capacity is quite complicated since this is mostly depended on engineer's experiences and mechanism of failure. One of the conservative methods is Davisson's method.

Brinch-Hansen method is in good agreements with real ultimate resistance of pile which gives about 80% of ultimate load calculated based on static loading test.

Chin-Kondner and Decourt methods both are using extrapolation for determination limit load values, hence, the ultimate load gained from both is asymptotically.

As a straight engineering rule never to interpret static loading test result to gain ultimate load larger than the test load. Therefore allowable load should not be calculated by dividing the limit loads obtained from Chin-Kondner's and Decourt's methods by a factor of safety.

The Mazurkiewicz method is easy to use and is more reliable especially for piles loaded near failure.

Shortcomings of De Beer's method are mentioned earlier. Hansen's 80%-criterion, Chin's and Decourt's

extrapolation methods using the latter part of the load-movement curve and could be extrapolated beyond the maximum load applied.

One of the advantages of Decourt's method is that a plot can be drawn while the static loading test is performing which allows the user to eyeball the projected capacity directly once a straight line plot starts to develop.

While in Chin-Kondner's method, if during the static loading test, a weakness in the pile develops, the curve would deviate from a straight line. Hence it is significantly desirable plotting the readings as per Decourt's method as the test progresses. Finally these two methods estimate ultimate failure load reasonably.

5. Conclusions

In this study, the behavior of helical piles with different helices in two sites with silty-clay and sandy soils was investigated. Moreover, the effect of grouting on pile's loading capacity was studied. The ultimate load capacity Q_u for each pile test was predicted using the six different interpretation methods that are used in the evaluation of the pile load test. The findings of this study can be summarized in the following conclusions:

- 1- Compressive capacity increased by approximately 8% after grouting. Similar to the single-helix piles, the pile resistance has increased by about 10% in the double-helix piles. But, in the triple-helix piles, the final load has been increased by about 28% after grouting.

- 2- grouting operation in clay had compaction performance, so loading capacity increased.

- 3- In triple-helix pile in silty-clayey soil, adhesion of pile and soil increased along with grouting. As a result, pile resistance was increased in comparison with the un-grouted condition.

- 4- Load-displacement curves showed that in sandy soil, the initial stiffness of the triple-helix piles was more than that of the double and single-helix piles, respectively.

- 5- In general, variation of pile strength with different helix numbers was insignificant. But the results of this paper indicated that grouting could considerably improve helical pile's strength.

Table 3: Summary of predicted ultimate failure loads

		Davisson	Hansen	Chin	Mazur	De Beer	Decourt	Test Site Load
		Qu(kN)	Qu(kN)	Qu(kN)	Qu(kN)	Qu(kN)	Qu(kN)	Qu(kN)
1 Helix	UngROUTed	22.5	54.55	53.19	54	12.18	53.7	50
	Grouted	32.5	73.7	63.7	64.9	16.44	61.98	58.9
2 Helix	UngROUTed	33.7	63.7	64.7	65.3	24.17	63.85	63.1
	Grouted	50.2	70.35	72.1	74	36.7	70.63	71.1
3 Helix	UngROUTed	66.2	73.7	77.1	78.3	60	75.4	76
	Grouted	104.7	113.2	115.8	116.3	94.47	114.25	114.8

6- According to various limit load methods evaluation, it was concluded that the values for three methods of Chin, Decourt were close to the site values.

- [7] American Society for Testing and Materials.; "Standard Test Methods for Deep Foundations Under Static Axial Compressive Load, ASTM D1143 / D1143M - 07"; Annu B ASTM Stand (2013) 04.08. doi:10.1520/D1143_D1143M.
- [8] Vickars R, Clemence S.; "Performance of Helical Piles with Grouted Shafts"; New Technol. Des. Dev. Deep Found., (2000) p. 327–41.

References

- [1] El Sharnouby MM, El Naggar MH.; "Field investigation of axial monotonic and cyclic performance of reinforced helical pulldown micropiles"; Can Geotech J (2012) 49:560–73. doi:10.1139/t2012-017.
- [2] Tsuha CHC, Aoki N, Rault G, Thorel L, Garnier J.; "Evaluation of the efficiencies of helical anchor plates in sand by centrifuge model tests"; Can Geotech J(2012) 49:1102–14. doi:10.1139/t2012-064.
- [3] Cerato AB, Victor R.; "Effects of Long-Term Dynamic Loading and Fluctuating Water Table on Helical Anchor Performance for Small Wind Tower Foundations"; J Perform Constr Facil (2009) 23:251–61. doi:10.1061/(ASCE)CF.1943-5509.0000013.
- [4] B.W. Byrne and G.T. Houlby; "Helical Piles: An Innovative Foundation Design Option for Offshore Wind Turbines"; (2016), J. Phil. Trans. R. Soc. A; 1-17. Doi: 10.1098/rsta.2014.008.
- [5] Abdelghany Y, El Naggar M.; "Full-Scale Field Investigations and Numerical Analyses of Innovative Seismic Composite Fiber-Reinforced Polymer and Reinforced Grouted Helical Screw Instrumented Piles Under Axial and Lateral Monotonic and Cyclic Loadings"; Adv. Soil Dyn. Found. Eng., (2014) p. 414–24. doi:10.1061/9780784413425.042.
- [6] Perko HA.; "Helical Piles, A Practical Guide to Design and Installation"; Hoboken, New Jersey: John Wiley and Sons, INC (2009).